THE JOURNAL OF BIOLOGICAL CHEMISTRY VOL. 283, NO. 20, pp. 13556–13564, May 16, 2008

Phage T5 Straight Tail Fiber Is a Multifunctional Protein Acting as a Tape Measure and Carrying Fusogenic and Muralytic Activities*

Received for publication, January 3, 2008, and in revised form, March 14, 2008 Published, JBC Papers in Press, March 17, 2008, DOI 10.1074/jbc.M800052200

Pascale Boulanger[‡§], Pierre Jacquot[‡§], Laure Plançon[‡§], Mohamed Chami[¶], Andreas Engel[¶], Claudine Parquet[‡§], Chantal Herbeuval[‡§], and Lucienne Letellier[‡§1]

From the [‡]Institut de Biochimie et Biophysique Moléculaire et Cellulaire, Université Paris-Sud, [§]CNRS, UMR 8619, Orsay F-91405, France, and [¶]ME Müller Institute, Biozentrum, University of Basel, Basel CH-4056, Switzerland

We report a bioinformatic and functional characterization of Pb2, a 121-kDa multimeric protein that forms phage T5 straight fiber and is implicated in DNA transfer into the host. Pb2 was predicted to consist of three domains. Region I (residues 1–1030) was mainly organized in coiled coil and shared features of tape measure proteins. Region II (residues 1030–1076) contained two α-helical transmembrane segments. Region III (residues 1135–1148) included a metallopeptidase motif. A truncated version of Pb2 (Pb2-Cterm, residues 964–1148) was expressed and purified. Pb2-Cterm shared common features with fusogenic membrane polypeptides. It formed oligomeric structures and inserted into liposomes triggering their fusion. Pb2-Cterm caused β-galactosidase release from *Escherichia coli* cells and *in vitro* peptidoglycan hydrolysis. Based on these multifunctional properties, we propose that binding of phage T5 to its receptor triggers large conformational changes in Pb2. The coiled coil region would serve as a sensor for triggering the opening of the head-tail connector. The C-terminal region would gain access to the host envelope, permitting the local degradation of the peptidoglycan and the formation of the DNA pore by fusion of the two membranes.

The mechanism by which the double-stranded DNA of tailed phages is transported through the envelope of Gram-negative bacteria is a complex process for which phages have developed diverse strategies. Transport may depend on transcription (T7) (1), on phage-encoded proteins (T7, T5, phi29) (1–3), and on host membrane potential (T4) (4, 5). The rate of DNA transport may also vary from phage to phage, reaching values as high as 3000–4000 bp/s (T4) or as low as 800 bp/s (T7) (reviewed in Refs. 6–8). Renewed attention was recently brought to these processes with studies focusing on the role of the capsid internal pressure as a trigger of DNA ejection (9) and on the structure of tail proteins participating in DNA ejection (10, 11) and with the development of single phage particles studies (12, 13). However, information on the *in vivo* DNA transport mechanism and on the phage/bacterial partners involved is still scarce.

The *Syphoviridae* coliphage T5 is an interesting example of the complex strategies developed by phages to invade bacteria. It consists of a 90-nm large icosahedral capsid containing a 121,750-bp double-stranded DNA and a 250-nm-long flexible tail. The high resolution structure of the T5 particle was recently solved from cryoelectron microscopy images highlighting two unusual characteristics of this phage: the triangulation number of its capsid ($t = 13$) and the 3-fold symmetry of its tail tube (14). Several other features make T5 an atypical phage (15). Its recently sequenced genome (GenBank™ accession numbers AY587007, AY692264, and AY543070 and Ref. 16) which is the largest among the T-odd viruses carries single-stranded interruptions at genetically defined positions on one of the DNA strands as well as large terminal redundancies in the form of 10,160-bp direct repeats (17). Another distinctive feature of T5 is the two-step transport of its genome (18). 8% of the DNA (FST[2] DNA) enters first the cytoplasm. A 4-min pause follows during which proteins encoded by this fragment are synthesized. Two of them (A1 and A2) then contribute to the transfer of the rest of the DNA (SST DNA) (2, 19). Numerous data have been collected on the interactions between the phage and its receptor (20, 21) but only few on the transport mechanism. T5 DNA transfer is initiated by reversible binding of the three L-shaped fibers to the O-antigen of the lipopolysaccharide, followed by irreversible binding of pb5, the receptor-binding protein, located at the distal end of the base plate to the iron-siderophore receptor FhuA (reviewed in Ref. 22). Then uncharacterized events lead to the opening of the capsid and the release of the DNA, which is transferred base pair after base pair through the host envelope. A transient efflux of cytoplasmic potassium accompanies DNA transport. We proposed that it corresponded to the insertion and transient opening in the cytoplasmic membrane of a pore through which the DNA was transferred (23). Fractionation of the envelope of T5-infected

* This work was supported in part by the CNRS program "Dynamique et Réactivité des Assemblages Biologiques" and by a Ph.D. fellowship from the Ministère de l'Education Nationale de la Recherche et de la Technologie (to P. J.). The costs of publication of this article were defrayed in part by the payment of page charges. This article must therefore be hereby marked "*advertisement*" in accordance with 18 U.S.C. Section 1734 solely to indicate this fact.

[1] To whom correspondence should be addressed: IBBMC, Bat 430, Université Paris Sud, Orsay, F-91405. Fax: 33-1-69-85-37-15; E-mail: lucienne.letellier@u-psud.fr.

[2] The abbreviations used are: FST, first step transfer; SST, second step transfer; LDAO, *N*,*N*-dimethyldodecylamine-*N*-oxide; MM, molecular mass; DDM, *n*-dodecyl-β-D-maltoside; TMP, tape measure protein; BN-PAGE, blue native polyacrylamide gel electrophoresis; LUV, large unilamellar vesicle(s); ONPG, *o*-nitrophenyl-β-D-galactopyranose; MALDI-TOF, matrix-assisted laser desorption ionization time-of-flight; Pb2-Cterm, truncated version of Pb2; HPLC, high pressure liquid chromatography.

Escherichia coli cells led us to conclude that Pb2, the protein forming the 50-nm-long straight tail fiber (24), probably formed the DNA pore (25), a conclusion compatible with data showing that Pb2 isolated from the phage particle had a pore-forming activity in planar lipid bilayers (26). Interestingly, cryo-electron microscopy and cryotomography images showed that the straight fiber could cross two lipid bilayers upon delivery of T5 DNA into proteoliposomes bearing the FhuA receptor and on which the phage was bound. Furthermore, the straight fiber underwent large conformational changes, appearing shorter and larger in the liposome than on the isolated phage (27–30). How Pb2 crosses successively the outer membrane and peptidoglycan and inserts into the cytoplasmic membrane to form a pore remains, however, speculative. To address these issues, we have performed an exhaustive analysis of the protein. Our data suggest that Pb2 not only forms the straight tail fiber but also fulfills the criteria of tape measure proteins. Furthermore, we show that its C-terminal region shares common features with fusogenic membrane peptides and carries a peptidoglycan hydrolase activity.

EXPERIMENTAL PROCEDURES

Bacterial Strains, Phages, Plasmids, and Growth Conditions—T5st0 was grown in the fast adsorbing strain *E. coli F* (31). The pET expression system (Novagen) with the pET-15b vector was used for overproduction of Pb2-Cterm in *E. coli* Bl21(DE3). The Zero Blunt TOPO PCR cloning kit (Invitrogen) was used for intermediate cloning steps. Except as otherwise indicated, bacteria were grown aerobically at 37 °C in LB medium.

Cloning Strategy—pb2-Cterm was amplified by PCR from T5st0 DNA using primers containing the NdeI and BamHI restrictions sites. The PCR product was purified and cloned into the pCR-BluntII-TOPO vector to generate TOPO*pb2-Cterm* that was amplified in TOP10 *E. coli* cells. The fragment encoding Pb2-Cterm was obtained by NdeI/BamHI restriction and inserted into the pET-15b expression vector. The final plasmid pCT4.4 encoded recombinant Pb2-Cterm fused to the His_6 N-terminal sequence MGSSHHHHHHSSGLVPRGS. All constructions were characterized by analysis with restriction nucleases and DNA sequencing.

Overexpression and Purification of Pb2-Cterm—E. coli BL21(DE3) carrying the pCT4.4 plasmid was grown to an $A_{600} = 0.8$ in LB supplemented with 100 μg/ml ampicillin. Pb2-Cterm expression was then induced with 0.4 mM isopropyl-β-D-thiogalactopyranoside. Cells were further grown for 2 h to an $A_{600} = 1$ and harvested by centrifugation (7000 × *g*, 4 °C, 10 min). The pellet was stored at −20 °C until protein extraction. Except as otherwise indicated, all further purification steps and experiments were carried out at room temperature and in the presence of complete protease inhibitor EDTA-free (Roche Applied Science). Frozen pellets (5 g) were suspended in 30 ml of 50 mM Tris, pH 8.0, 150 mM NaCl, 5 μg/ml DNase, 2 mM $MgCl_2$. Cells were broken by three runs through a French press at 14,000 p.s.i. and centrifuged (5000 × *g*, 4 °C, 15 min). The pellet containing Pb2-Cterm was suspended in 30 ml of 50 mM Tris, pH 8.0, 1% (w/v) LDAO for 1 h and centrifuged (10,000 × *g*, 4 °C, 15 min). The supernatant was loaded onto a column packed with 18 ml of Superflow nickel-nitrilotriacetic acid resin (Qiagen) equilibrated with 50 mM Tris, pH 8.0, 0.1% LDAO and adapted to an Ákta chromatography system (GE Healthcare). Pb2-Cterm was eluted at 750 mM imidazole and further purified by anion exchange chromatography on Resource Q, which also allowed exchanging LDAO for DDM. Pb2-Cterm was selectively eluted at 390 mM NaCl and finally stored in 25 mM Tris, pH 7.8, 150 mM NaCl, 0.1% DDM, 0.02% NaN_3. The yield of purified Pb2-Cterm was 10 mg/liter culture. For purification of Pb2-Cterm from membranes, the supernatant recovered from the low speed centrifugation of French press-broken bacteria was centrifuged (100,000 × *g*, 4 °C, 30 min). The pellet was suspended for 1 h at 4 °C in 50 mM Tris, pH 8, 1% LDAO and centrifuged at 100,000 × *g* to remove the insoluble material. The supernatant was further purified in two steps as described above for cytoplasmic Pb2-Cterm.

Bioinformatic Analysis—Secondary structure prediction was according to GOR4 (32). Coiled coil prediction was according to Ref. 33 and using the COILS2 program. Transmembrane domains were predicted using SOSUI (34). Sequence homologies were searched using PSI-BLAST (35). PROSITE was used to investigate conserved motifs (36). Annotation of phage T5 tail genes was according to GenBank accession number AY692264. The Pb2 sequence was according to GenBank accession number AY303686.

Pb2-Cterm Characterization by Size Exclusion Chromatography and Measurement of Bound Detergent—Pb2-Cterm eluted from the Resource Q column was applied onto a Superose 12 HR 10/30 column equilibrated with 25 mM Tris, pH 7.8, 150 mM NaCl, 0.1% DDM (Superose buffer). Elution was carried out at a flow rate of 0.25 ml/min. For estimation of the apparent MM (MM_{app}), the column was calibrated using the following proteins of known Stokes radius solubilized in Superose buffer: thyroglobulin (8.6 nm), ferritin (6.3 nm), catalase (5.2 nm), aldolase (4.6 nm), bovine serum albumin (3.5 nm), ovalbumin (2.8 nm), chymotrypsinogen (2.1 nm), and ribonuclease A (1.75 nm) (37). Dextran Blue 2000 and $NaNO_3$ (80 mM) were used as markers of void volume and total column volume, respectively. For measurement of bound detergent, purified Pb2-Cterm was loaded onto the Superose column equilibrated in Superose buffer containing [1-^{14}C]DDM (2 mM; 0.6 MBq/mmol). Fractions containing Pb2-Cterm were pooled and reloaded on the same column to ensure complete exchange of cold for [1-^{14}C]DDM. Collected fractions were counted for detergent radioactivity, and the Pb2-Cterm concentration was determined using the extinction coefficient deduced from the protein sequence (7680 M^{-1} cm^{-1} at 280 nm).

BN-PAGE—Experiments were performed essentially as described (38). 5 μg of Pb2-Cterm in 25 mM Tris, pH 7.8, 150 mM NaCl containing variable concentrations of DDM (0.02–0.2%) were applied onto a 5–18% (w/v) polyacrylamide gradient gel. Samples were supplemented with the loading dye (5% Commassie Brilliant Blue, 500 mM 6-amino-*n*-caproic acid, and 100 mM Bis-Tris, pH 7.0). Gels were stained with Commassie Brilliant Blue. The MM_{app} was calculated using the following relationship: $M_{BNP} = 1.8 \times M_{AA}$, where M_{AA} and M_{BNP} represent the MM of the protein based on its amino acid sequence and on BN-PAGE, respectively (39). M_{BNP} was estimated using the fol-

lowing mass markers: α-chymotrypsin (43 kDa), BSA (67 kDa), aldolase (158 kDa), and ferritin (440 kDa).

Electron Microscopy and Single Particle Analysis—Pb2-Cterm (20 μM) purified from membrane fractions was 10-fold diluted in 20 mM Tris, pH 7.5, 0.02% DDM. Aliquots (5 μl) were applied onto a glow-discharged carbon-coated grid and stained with 2% (w/v) uranyl acetate. Micrographs were recorded at a magnification of ×50,000 using a Hitachi 7000 electron microscope operating at 100 kV. Micrographs were recorded on Eastman Kodak Co. SO-163 films and digitized with a Primescan (Heidelberg, Germany) at a resolution of 5 Å/pixel at the specimen level. Reference-free alignment was performed on manually selected particles from digitized electron micrographs using the EMAN image processing package (40). Particle projections were classified by multivariant statistical analysis. The class particles with the best signal-to-noise ratio were selected.

Assays of Pb2-Cterm Activity in Liposomes—LUV were prepared by sequential extrusion through 0.8-, 0.4-, and 0.2-μm polycarbonate membranes (Nucleopore) of a soybean phosphatidylcholine and phosphatidic acid suspension (molar ratio 9:1) in 25 mM sodium phosphate buffer, pH 7.2 (27). The lipid concentration was determined by adding a trace amount of [^{14}C]phosphatidylcholine (4.1×10^8 Bq/mmol, 18.5 kBq/ml). For reconstitution into liposomes, 10 μg of Pb2-Cterm were added to 8 mg of the phosphatidylcholine/phosphatidic acid mixture suspended in 100 μl of 25 mM sodium phosphate buffer, pH 7.2, 2% octyl-β-D-glucopyranoside (w/v). After 1 h of incubation, the detergent was slowly removed using Biobeads (Bio-Rad) (41). For floatation sucrose gradients, the suspensions consisting of liposomes, of Pb2-Cterm either alone or incubated with the liposomes (Pb2-Cterm/lipid molar ratio 1:900), or of Pb2-Cterm reconstituted into the liposomes were adjusted to 34% sucrose by mixing with a 78% sucrose solution in 25 mM sodium phosphate buffer, pH 7.2. Samples were deposited at the bottom of a sucrose gradient and overlaid with successive sucrose layers up to 11%. For assays with Pb2-Cterm alone, the sucrose solutions contained 0.1% DDM. After centrifugation (4 °C, 90 min, 100,000 × *g*) fractions were collected from the top. Lipids were counted for radioactivity and the protein content was determined by densitometry of a silver-stained SDS-PAGE.

The time-dependent changes of the light scattered by the LUV upon the addition of variable concentrations of Pb2-Cterm were measured from the absorbance of the suspension at 400 nm. Liposomes were suspended in 25 mM sodium phosphate buffer, pH 7.2, at a concentration of 275 μM. For determination of their hydrodynamic radius by dynamic light scattering, LUV were preincubated with Pb2-Cterm for 1 h (protein/lipid molar ratio 1:360) before measurements with a particle size analyzer (Brookhaven).

Efflux of β-Galactosidase from E. coli Cells and Pb2-Cterm Bactericidal Activity—Exponentially grown *E. coli* ML 35 cells were harvested, washed, and suspended to an $A_{600} = 0.1$ (1×10^8 cells/ml) in 25 mM sodium phosphate buffer, pH 7.2. Pb2-Cterm (3 μM final concentration) was added to 1 ml of the cell suspension, incubated for variable times at 37 °C, and centrifuged at 8000 × *g*. Released β-galactosidase was assayed by mixing 500 μl of the supernatant with an equal volume of ONPG (1.5 mM final concentration). Hydrolysis of ONPG was measured from the absorbance at 420 nm. The β-galactosidase activity was compared with that of the supernatant of an equivalent amount of bacteria broken by sonication. For measurement of Pb2-Cterm bactericidal activity, *E. coli* ML 35 cells were prepared as described above. 1×10^7 cells were mixed with variable concentrations of Pb2-Cterm, incubated for 30 min at 37 °C, and plated for determination of their survival.

Pb2-Cterm Activity on Muropeptides—Peptidoglycan was extracted from *E. coli* cells and purified as described (42). For measurements of activities, 1 nmol of Pb2-Cterm was incubated with 200 nmol of purified peptidoglycan in 0.1 ml of 20 mM sodium phosphate buffer, pH 7.2, 0.1% DDM for 1 h at 37 °C. Peptidoglycan samples treated or not with Pb2-Cterm were then digested by mutanolysin (250 μg/ml) for 16 h at 37 °C in 100 μl of potassium phosphate buffer, pH 6.5. Muropeptides were further reduced and purified by reverse HPLC on a C18 Hypersil column 3μ. Elution was made with a linear gradient of acetonitrile (eluent A: 0.05% trifluoroacetic acid; eluent B: 0.04% trifluoroacetic acid plus 20% acetonitrile (*V/V*); 0 to 100% B in 60 min). Fractions were detected from the absorbance at 210 nm. They were identified by MALDI-TOF mass spectrometry and analysis of amino acids and amino sugars.

RESULTS

Bioinformatic Analysis of Pb2—pb2 (3844 bp) belongs to the late class of genes and is located within the region of the genome encoding most of the head and tail structural genes. Pb2 accounts for about 1.5% of the total mass of T5 structural proteins (43), leading to an estimate of 5–6 copies in a phage particle (15). Pb2 is the unique T5 tail protein that is processed by proteolytic cleavage during morphogenesis (44). N-terminal sequencing and mass spectrometry (MALDI-TOF) of Pb2 isolated from T5 ghosts led us to conclude that maturation was at the C-terminal end, resulting in a polypeptide of 123.9 ± 0.1 kDa (cleavage site after Val^{1148} (±1)) (data not shown).

A bioinformatic analysis allowed identifying three regions in mature Pb2. Region I (residues 1–1030) was mainly organized in coiled coil, with the highest scores found for seven regions (residues 19–46, 434–477, 499–526, 659–707, 869–889, 915–942, and 1003–1030 (Fig. 1*A*). Such high coiled coil content is characteristic of TMP (45). Recent studies have revealed that the TMP genes of numerous *Siphoviridae* phages are located downstream and upstream those encoding the major tail and base plate proteins, respectively (46, 47). Such organization was also found in T5, since *pb2* was found downstream the genes encoding the major tail protein pb6 (*p141*) and a putative tail terminator (*p142*) identified by alignment with phage λ terminator gpU (48). *pb2* was also located upstream the genes encoding the two putative base plate proteins Pb3 and Pb4 (20). Following this predicted coiled coil region, we found a domain rich in hydrophobic residues. Hydropathy profiles according to SOSUI (34) predicted two helical transmembrane-spanning segments (residues 1030–1052 and 1054–1076). In addition, this region contained numerous alanines and glycines (16 over 44 residues), two amino acids that are important for triggering fusogenic processes (Fig. 1*B*) (49). In contrast to these two regions, which showed a high propensity to fold as

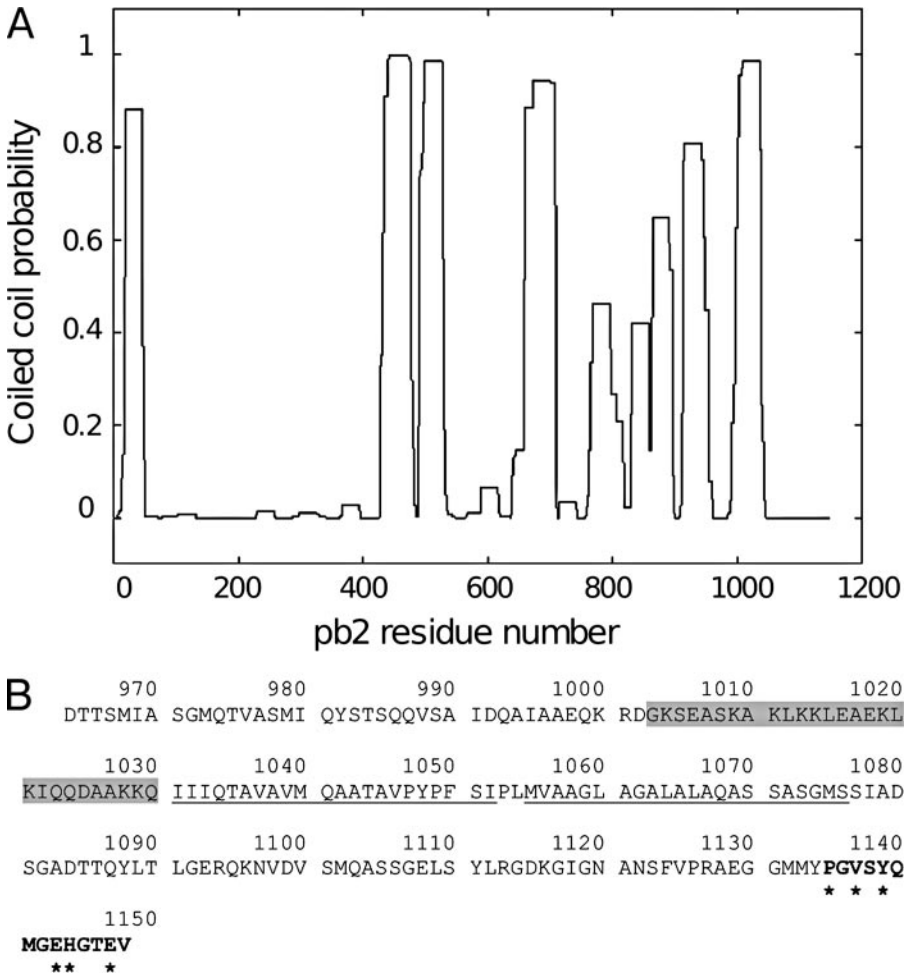

FIGURE 1. **Bioinformatic analysis of Pb2.** *A*, prediction of coiled coil motifs in mature Pb2. Prediction was according to the COILS2 program and using a 28-residue window width. Probability scores are on a scale of 0–1. Regions that show the highest scores extended from residues 19 to 46, 434 to 477, 499 to 526, 659 to 707, 869 to 889, 915 to 942, and 1003 to 1030. *B*, Pb2-Cterm primary sequence. The predicted coiled coil domain (residues 1003–1030) is delimited by the *gray shaded region*. The membrane-spanning α-helices (residues 1030–1052 and 1054–1076) are *underlined*. The zinc metallopeptidase motif is in *boldface type*. Conserved residues resulting from a Prosite analysis (PS00132) are shown as *stars*.

α-helices (69.9%), the C-terminal region was predicted to be essentially random coil. It included a short segment (residues 1135–1148) that is very similar to a zinc metallopeptidase motif (Fig. 1*B*).

Cloning, Expression, and Purification of Pb2-Cterm, a Truncated Version of Pb2—The purification of Pb2 by treatment of isolated phage tails with 0.05% SDS was previously described (26). However, whatever the modifications brought to the protocol, we failed to recover a preparation pure enough and in sufficient amount to conduct its characterization. Overproducing Pb2 in *E. coli* led to inclusion bodies that could badly be recovered in a soluble and refolded state when submitted to various denaturation/renaturation procedures. Since we aimed at deciphering whether and how Pb2 interacted with the *E. coli* envelope, we focused on the expression of a truncated version of Pb2 (Pb2-Cterm, 185 residues: Asp^{964}–Val^{1148}) encompassing one of the predicted coiled coil region, the transmembrane-spanning segments, and the metallopeptidase motif (Fig. 1*B*). Overexpression in *E. coli* of Pb2-Cterm carrying a His_6 in the N terminus caused growth arrest, suggesting that the protein was toxic. Pb2-Cterm was targeted to both the membranes and the cytoplasm. The cytoplasmic fraction formed aggregates that could be solubilized by LDAO. LDAO also extracted the protein from the membranes. Further two-step purification of Pb2-Cterm from both fractions led to a unique polypeptide displaying an electrophoretic mobility of ~20 kDa compared with 21 kDa calculated from the sequence. Except where otherwise indicated, experiments were conducted with the protein originating from the cytoplasmic fraction, since its yield was higher than that of the membrane fraction.

Pb2-Cterm migrated as a broad peak in size exclusion chromatography, whether isolated from the cytoplasm (Fig. 2*A*) or from the membranes (not shown). The position of the peak remained unchanged for concentrations up to 177 μM (Fig. 2*A*) but was shifted toward the exclusion volume above this concentration, indicating that aggregated species were formed (not shown). The Stokes radius estimated at the peak maximum for the three concentrations tested (42, 89, and 177 μM) was 5.2 nm. Assuming the protein to be roughly globular (see electron microscopy pictures, Fig. 3), this corresponded to a MM_{app} of 220 $\pm$ 20 kDa. This value includes the MM of the protein and that of the bound detergent. Detergent binding was estimated from the size exclusion chromatogram using [1-^{14}C]DDM (50, 51). The elution profile of radioactive DDM was superimposed onto that of Pb2-Cterm (Fig. 2*A*), an indication of the strong association of the detergent to the protein. From the elution profiles, we calculated a detergent to protein molar ratio of 45 $\pm$ 5, corresponding to a MM of a Pb2-Cterm monomer with its detergent of 44.5 kDa. Given the MM_{app} at the peak maximum (220 $\pm$ 20 kDa), this implies that Pb2-Cterm is mainly pentameric. However, the broadness of the peak suggests that this pentamer coexists with other oligomerization states. This was confirmed by a BN-PAGE analysis. Pb2-Cterm migrated at five positions that remained unchanged whatever the concentration of DDM used between 0.02 and 0.2% (data not shown), an indication that stable oligomers were formed (39). Their MM_{app} was estimated after appropriate corrections for detergent/dye binding. They corresponded to increasing oligomerization states from the monomer (a minor form), up to the pentamer (Fig. 2*B*).

The membrane-extracted form of Pb2-Cterm eluted by size exclusion chromatography was imaged by negative stain elec-

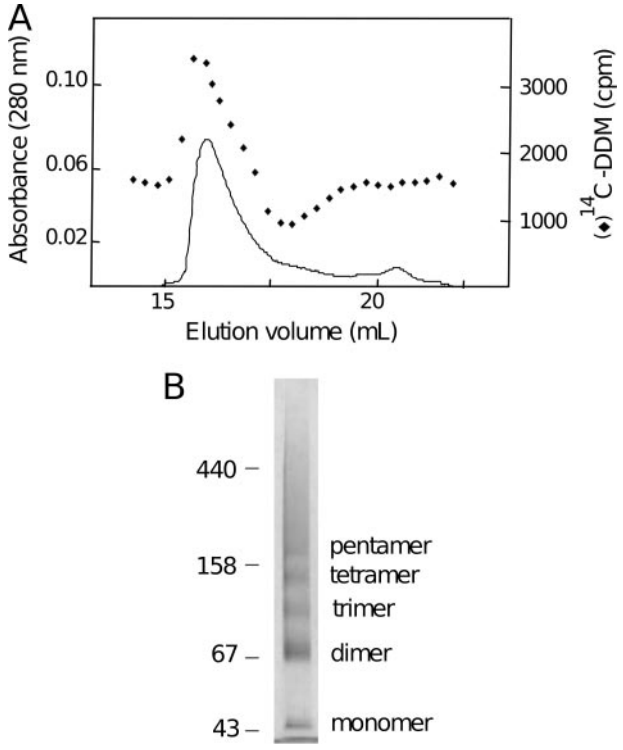

FIGURE 2. **Oligomerization states of Pb2-Cterm.** *A*, the size exclusion chromatogram of Pb2-Cterm (89 μM) on Superose 12 (*solid line*) and the elution profile of bound [1-^{14}C]DDM (*diamond*) are superimposed. *B*, BN-PAGE showing the different states of oligomerization of Pb2-Cterm in 25 mM Tris, pH 7.8, 150 mM NaCl containing 0.1% DDM. *Left lane*, MM markers. The bands are consistent with the monomer, dimer, trimer, tetramer, and pentamer forms of Pb2-Cterm. Their MM_{app} values were calculated as described under "Experimental Procedures."

tron microscopy. Fig. 3 represents an overview of the 1700 particles analyzed. Many of them formed large globular structures. Their mean diameter (10 ± 1 nm) was compatible with an organization in pentamer/hexamer, but their size and the resolution obtained precluded a clear analysis of their symmetry. Smaller particles were occasionally observed that might correspond to lower states of oligomerization, but their size did not allow a quantitative analysis. Altogether, the above data suggest that Pb2-Cterm, whether extracted from the cytoplasm or the membranes, exists in different states of association barely separable from each other and possibly in equilibrium.

Pb2-Cterm Is a Membrane-acting and Fusogenic Polypeptide—We first evaluated the capacity of Pb2-Cterm to interact with lipids by determining the location of the protein on a floatation sucrose gradient (Fig. 4). Pb2-Cterm remained at the bottom of the gradient in the absence of lipids but co-migrated with the lipids when preincubated with LUV. Furthermore, when we applied a protocol that is used for reconstitution of membrane proteins into liposomes (41), Pb2-Cterm and lipids co-migrated, an indication that the protein was indeed reconstituted into the LUV. Interestingly, the addition of Pb2-Cterm to LUV resulted in an increase of the light scattered by the liposomes. Its amplitude rose with the Pb2-Cterm concentration and reached a plateau in about 10 min (Fig. 5). This increase, which was not observed with the liposomes or the protein alone, was accompanied by an increase the hydrodynamic radius (R_h) of

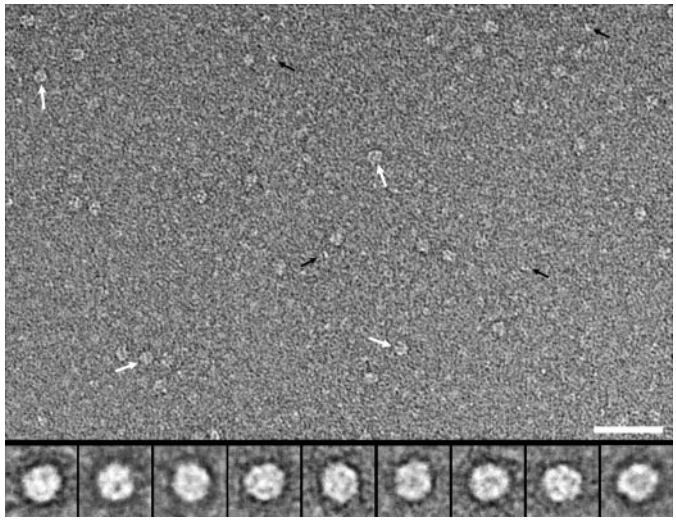

FIGURE 3. **Electron microscopy images of negatively-stained Pb2-Cterm.** Pb2-Cterm concentration was 2 μM. Micrographs were recorded at a magnification of ×50,000. *Bar*, 40 nm. The *white arrows* indicate the largest particles. The *black arrows* correspond to lower states of oligomerization. The *insets* display class averages of a total of 1700 hand-picked images, representing different orientations of the particles on the carbon support. The base lines correspond to 15 nm.

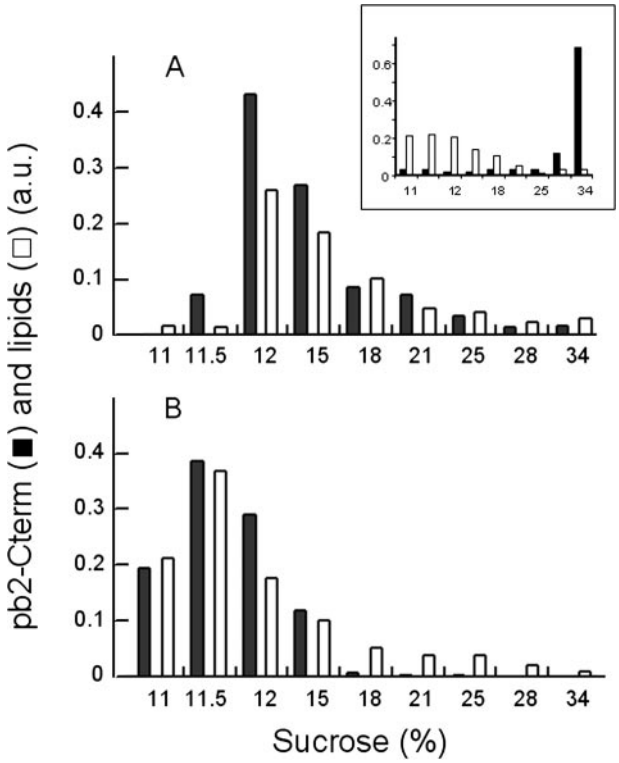

FIGURE 4. **Localization of Pb2-Cterm and liposomes on floatation sucrose gradients.** Pb2-Cterm either incubated with LUV made of phosphatidylcholine and phosphatidic acid (molar ratio 9:1) at a protein/lipid molar ratio of 1:900 (*A*) or reconstituted into the LUV (*B*) were deposited at the bottom of a sucrose gradient overlaid with successive sucrose layers up to 11%. The lipid and protein content of the collected fractions was estimated from their radioactivity and by densitometry of a silver-stained SDS-PAGE, respectively, and was expressed in arbitrary units (a.u.). *Inset*, control experiments showing the migration of Pb2-Cterm and of liposomes alone.

the LUV from 160 ± 20 nm (mean value of 1400 particles) to 250 ± 20 nm (mean value of 1000 particles) for LUV incubated with Pb2-Cterm at a protein/lipid molar ratio of 1:360.

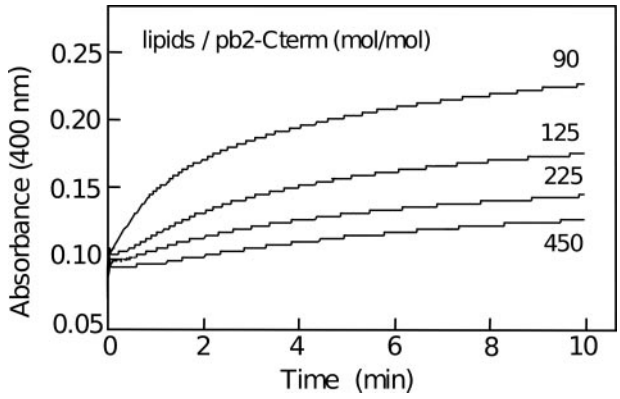

FIGURE 5. **Pb2-Cterm triggers an increase of the light scattered by liposomes.** Pb2-Cterm was added to the LUV at the lipid/protein molar ratio indicated, and the absorbance was measured at 400 nm. The light scattered by the liposomes was subtracted from the base line. The contribution of DDM present with the protein was negligible.

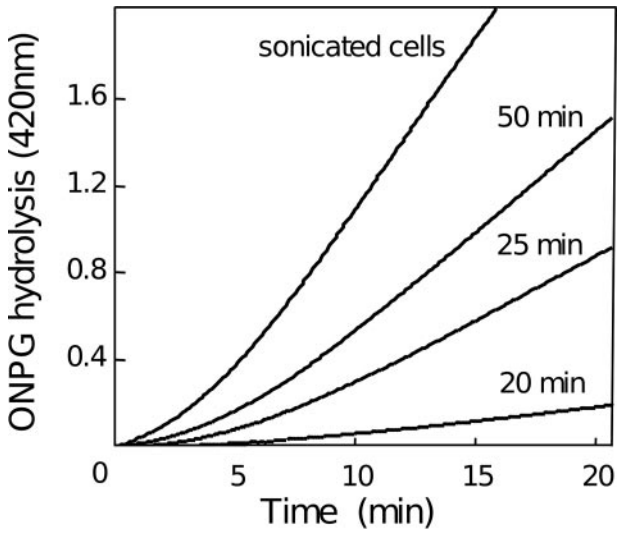

FIGURE 6. **Efflux of β-galactosidase from *E. coli* cells induced by Pb2-Cterm.** *E. coli* cells (1×10^8 cells/ml) were incubated at 37 °C with Pb2-Cterm (3 μM). Released β-galactosidase was assayed by measuring the hydrolysis of ONPG at 420 nm in the supernatant of bacteria treated with Pb2-Cterm for the times indicated. Total β-galactosidase was estimated on an equivalent amount of sonicated bacteria.

This increase is most likely due to fusion of the liposomes rather than to their aggregation, since the distribution of particles was unimodal. Altogether, these results suggest that Pb2-Cterm behaves similarly to membrane-active fusogenic peptides.

In Vivo Activity of Pb2-Cterm—In an attempt to decipher Pb2-Cterm *in vivo* target(s), we conducted several functional assays. *E. coli* cells treated with 3 μM Pb2-Cterm released cytoplasmic β-galactosidase, as judged by the hydrolysis of ONPG measured in the cell supernatant (Fig. 6). After a 50-min incubation, released β-galactosidase reached about 60% of the level attained with sonicated bacteria. β-Galactosidase efflux was not due to DDM, since its addition, even in large excess compared with the amount added with the protein, did not cause any release of β-galactosidase (not shown).

Triggering the efflux of such large molecules from the cytoplasm required that Pb2-Cterm had crossed both membranes

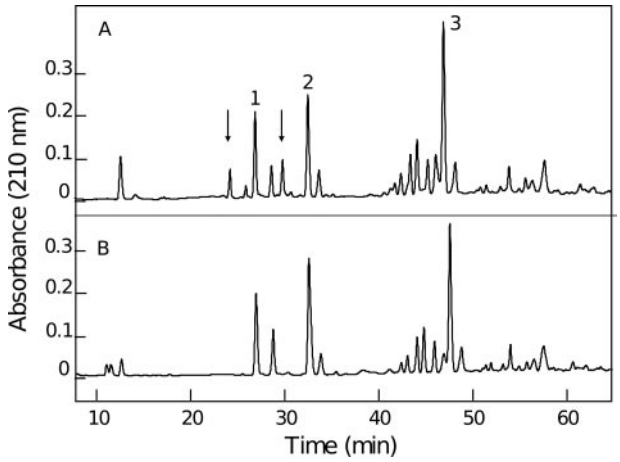

FIGURE 7. **Peptidoglycan hydrolase activity of Pb2-Cterm.** HPLC chromatograms of muropeptides resulting from digestion by mutanolysin of purified *E. coli* peptidoglycan incubated (*A*) or not (*B*) with Pb2-Cterm. Absorbance was measured at 210 nm. *Fractions 1–3* correspond to the disaccharide-tripeptide, disaccharide-tetrapeptide, and dimer of the disaccharide-tetrapeptide, respectively. The *arrows* indicate the new digestion products formed by incubation of Pb2-Cterm with peptidoglycan.

and the peptidoglycan. We therefore asked whether Pb2-Cterm carried a peptidoglycan hydrolase activity. Digestion of purified peptidoglycan by mutanolysin specifically generated three major species: a disaccharide-tripeptide, a disaccharide-tetrapeptide, and the dimer of the disaccharide-tetrapeptide. This HPLC profile was significantly modified if peptidoglycan was first incubated with Pb2-Cterm and then digested with mutanolysin, since new digestion products appeared besides those expected (Fig. 7). Since Pb2-Cterm by itself had no effect on the isolated peptides generated by mutanolysin (not shown), this suggests that the protein is able to degrade, at least partially, the peptidoglycan.

In brief, Pb2-Cterm had a bactericidal effect on *E. coli* cells. This was attested by plating bacteria treated with the protein as described above; 98% of the bacteria were killed when incubated with Pb2-Cterm at a concentration of >3 μM.

DISCUSSION

This study sheds some light on the mechanism underlying the conversion of phage T5 straight tail fiber Pb2 from a phage-attached protein to a membrane-active polypeptide. The first part of this work focused on the analysis of Pb2 sequence. As stated in numerous studies, there is a lack of identity among phage structural genes, making it difficult to identify a given protein from primary sequence comparisons (46, 52). Pb2 was not an exception to this rule, since all BLAST searches remained unsuccessful. However, several arguments led us to conclude that Pb2 fulfills the criteria characterizing TMP. (i) The Pb2 location on the tail gene module matches well that of the TMP genes from *Siphoviridae* phages. (ii) Pb2 is among the largest tail genes, encoding a 1148-residue mature protein, and a large majority of the Pb2 N-terminal region is predicted to be in coiled coil. Accordingly, this enables this region of the protein, if in an extended helical conformation, to span the 250-nm-long tail tube (45, 53). (iii) Pb2 shares common features with phage λ TMP (gpH); the number of Pb2 and gpH proteins in the phage particle are identical (5 to 6), and they are matu-

rated by proteolytic cleavage in C-terminal during phage assembly (reviewed in Ref. 54). Altogether, this suggests that Pb2 both forms the straight fiber (24) and spans the phage tail. This situation is different from that found in phage λ, whose TMP and straight fiber correspond to two different proteins, gpH and gpJ, respectively (55–57). How is the T5 tail then assembled? We can reasonably assume that Pb2, like gpH, is part of the initiation complex required for polymerization of the major tail protein, pb6. In λ, gpJ assembles first, followed by gpH (58). Whether Pb2 assembles to handle either functions or whether other proteins participate in tail polymerization remains to be determined. The organization of T5 tail genes differs from that of *Siphoviridae* λ phages. Indeed, a translational frameshift is strongly conserved in tail assembly genes of double-stranded DNA phages, arguing for its fundamental role. In phage λ, this frameshift controls the production of two proteins with overlapping sequences, gpG and gpT, that are located downstream from the major tail protein gene and upstream from the TMP gene (59). We failed to identify such frameshift sites in the corresponding region of T5 tail genes. T5 also differs from *Siphoviridae* λ phages by the location of the receptor binding protein, pb5, whose gene (*p153*) is not located in the tail module but shifted toward the capsid module, beyond the terminase genes. Finally, the T5 tail, unlike those of most known phages, which are 6-fold symmetric, is 3-fold symmetric (14). Overall, this highlights the peculiar character of T5 and makes this phage an interesting model for assembly studies.

Previous studies have shown that binding of T5 to its receptor FhuA results in the insertion of Pb2 in the host membranes (25) and in liposomes reconstituted with FhuA (30). Since the C terminus of Pb2 was the only region predicted to contain helical transmembrane-spanning segments, it was reasonable to assume its implication in membrane insertion. Expression in *E. coli* of a truncated version of Pb2 (Pb2-Cterm, 185 residues) including this region indeed showed that the polypeptide had all features of a membrane protein. It was recovered in the cytoplasm as aggregates and in membranes. Both forms could easily be solubilized by a zwitterionic or neutral detergent and showed similar characteristics. The amount of detergent they bound (45 mol/mol of protein) was compatible with the size of their hydrophobic sectors (50). Size exclusion chromatography and BN-PAGE indicated that Pb2-Cterm existed in different oligomerization states up to the pentamer barely separable from each other, thus probably in equilibrium. These data were corroborated by electron microscopy observations showing that Pb2-Cterm formed large globular structures, whose size was compatible with an organization in pentamer or hexamer. In conclusion, the oligomerization state of the truncated polypeptide is relevant to that of Pb2 in the phage particle (5–6 copies) (43).

Pb2-Cterm showed multiple interesting features *in vitro*. It inserted spontaneously into liposomes and could be reconstituted into lipid vesicles, further attesting to its behavior as a membrane protein. Pb2-Cterm also triggered an increase of the light scattered by the liposomes and of their mean hydrodynamic radius, suggesting that it had a fusogenic activity. This fusogenic activity was noticeable at a protein/lipid molar ratio as low as 1:360. This fusion probably occurred via the region predicted to span the membranes, which contains a high amount of alanine and glycine, two amino acids that are important for triggering fusogenic processes (49).

Pb2-Cterm was also active *in vivo* triggering the release of cytoplasmic β-galactosidase and being *in fine* bactericidal. The concentration of Pb2-Cterm causing irreversible damages was 3 μM. As stated above, Pb2-Cterm exists in different oligomerization states, making it difficult to determine which of the polypeptide states is (are) active and what its concentration is in the host envelope. It should be stressed that this is a recurrent situation with antibacterial peptides (60). Such severe effects require that Pb2-Cterm had crossed both membranes and the peptidoglycan. The crossing of membranes most likely involves the two transmembrane segments and takes place independently of receptor recognition, since Pb2-Cterm inserted spontaneously into liposomes. Peptidoglycan activity was attested by degradation of purified peptidoglycan. This muralytic activity is most probably due to the short metallopeptidase motif located at the very end of the Pb2-Cterm sequence. Cell wall-degrading activities have been identified or characterized in phages structural proteins at the initiation of infection and upon cell lysis (61–63). It was suggested that T5 phage contained a 33-kDa structural protein with muralytic activity (63). However, neither the analysis of the T5 genome nor that of its structural proteins (43) allowed us to identify this protein. Interestingly, the TMP from TM4, a *Syphoviridae* mycobacteriophage contains a short motif that has a peptidoglycan-hydrolyzing activity. This motif is also found in TMP of phages infecting a large variety of Gram-positive bacteria, suggesting that they use a common strategy for crossing the cell wall (64). Whether TMP peptidoglycan-hydrolyzing activity is conserved among *Syphoviridae* phages from Gram-negative bacteria remains an open question.

Overall, our results strongly suggest that Pb2 plays several roles in the phage and in its host. In the phage particle, Pb2 would be in an extended conformation with its coiled coil region spanning the tail and its fusogenic C-terminal region sequestered within the distal part of the tail, presumably in the straight fiber. Binding of T5 to FhuA via its receptor-binding protein, pb5, would generate major changes in Pb2; the coiled coil domain would serve as a sensor for triggering the opening of the head-tail connector, and the release of the DNA from the capsid and the C-terminal region would gain access to the outer membrane. These conformational changes are attested by cryotomography images of T5 interacting with FhuA-bearing liposomes (30) and by former observations showing that Pb2 becomes sensitive to proteolysis when isolated T5 tails interact with FhuA (26). These conformational changes would result in local degradation of the peptidoglycan and formation of a pore by fusion of the outer and inner membranes. Fusion would serve two purposes: ensuring the contact between the two membranes so as to protect the DNA from periplasmic nucleases and forming the DNA pore. Given the number of Pb2 copies in the phage particle (5 to 6) this pore might be large enough for the

DNA to go through. Whether Pb2 is fully injected into the host envelope or remains attached to the phage is not clear. *In vivo* Pb2 is found associated with the bacterial envelope upon DNA transfer (25). *In vitro* the straight tail fiber crosses the liposome membrane when DNA is injected but remains attached to the phage tail (30). Another unsolved question is related to the peculiar two-step mechanism of DNA transport. We previously observed that the efflux of cytoplasmic potassium, which occurs concomitantly with DNA transfer, ceased after injection of FST DNA and started again after synthesis of FST-encoded proteins and transfer of the SST DNA (23). This suggested that the pore would open first upon FST DNA transfer and then close during the synthesis of the FST-encoded proteins and again transiently reopen during the transfer of the SST DNA. The trigger for pore closing could be the interaction of the pore-forming domain of Pb2 with the region of the FST DNA characterized by potential stem-and-loop structures and corresponding to inverted repeats and palindromic sequences (65). The possibility of handling a pure membrane-active protein might provide *in vitro* conditions for determination of whether it is able to recognize specific DNA sequences.

Acknowledgments—We gratefully acknowledge C. Breyton and A. Huet for advice and P. Decottignies for protein sequencing.

REFERENCES

1. Molineux, I. J. (2001) *Mol. Microbiol.* **40,** 1–8
2. McCorquodale, D. J., Shaw, A. R., Shaw, P. K., and Chinnadurai, G. (1977) *J. Virol.* **22,** 480–488
3. Gonzalez-Huici, V., Salas, M., and Hermoso, J. (2004) *Mol. Microbiol.* **52,** 529–540
4. Labedan, B., and Goldberg, E. B. (1979) *Proc. Natl. Acad. Sci. U. S. A.* **76,** 4669–4673
5. Goldberg, E., Grinius, L., and Letellier, L. (1994) in *Molecular Biology of Bacteriophage T4* (Karam, J. D., ed) pp. 347–356, American Society of Microbiology, Washington, DC
6. Letellier, L., Boulanger, P., De Frutos, M., and Jacquot, J. P. (2003) *Res. Microbiol.* **154,** 283–287
7. Letellier, L., Boulanger, P., Plancon, L., Jacquot, P., and Santamaria, M. (2004) *Front. Biosci.* **9,** 1228–1339
8. Letellier, L., Plancon, L., and Boulanger, P. (2007) in *Bacteriophage*: *Genetics and Molecular Biology* (McGrath, S., ed) pp. 209–228, Caster Academic Press, Norfolk, UK
9. Inamdar, M. M., Gelbart, W. M., and Phillips, R. (2006) *Biophys. J.* **91,** 411–420
10. Plisson, C., White, H. E., Auzat, I., Zafarani, A., Sao-Jose, C., Lhuillier, S., Tavares, P., and Orlova, E. (2007) *EMBO J.* **26,** 3720–3728
11. Olia, A., Casjens, S., and Cingolani, G. (2007) *Nat. Struct. Biol.* **14,** 1221–1226
12. Mangenot, S., Hochrein, M., Radler, J., and Letellier, L. (2005) *Curr. Biol.* **15,** 1–20
13. Grayson, P., Han, L., Winther, T., and Phillips, R. (2007) *Proc. Natl. Acad. Sci. U. S. A.* **104,** 14652–14657
14. Effantin, G., Boulanger, P., Neumann, E., Letellier, L., and Conway, J. (2006) *J. Mol. Biol.* **361,** 993–1002
15. McCorquodale, J. D., and Warner, H. R. (1988) in *The Viruses* (Calendar, R., ed) Vol. 1, pp. 439–476, Plenum Press, New York
16. Wang, J., Jiang, Y., Vincent, M., Sun, Y., Yu, H., Bao, Q., Kong, H., and Hu, S. (2005) *Virology* **332,** 45–65
17. Rhoades, M., and Rhoades, E. A. (1972) *J. Mol. Biol.* **69,** 187–200
18. Lanni, Y. T. (1968) *Bacteriol. Rev.* **32,** 227–242
19. Snyder, C. E., Jr., and Benzinger, R. H. (1981) *J. Virol.* **40,** 248–257
20. Feucht, A., Heinzelmann, G., and Heller, K. J. (1989) *FEBS Lett.* **255,** 435–440
21. Plançon, L., Janmot, C., le Maire, M., Desmadril, M., Bonhivers, M., Letellier, L., and Boulanger, P. (2002) *J. Mol. Biol.* **318,** 557–569
22. Heller, K. J. (1992) *Arch. Microbiol.* **158,** 235–248
23. Boulanger, P., and Letellier, L. (1992) *J. Biol. Chem.* **267,** 3168–3172
24. Heller, K. J., and Schwarz, H. (1985) *J. Bacteriol.* **162,** 621–625
25. Guihard, G., Boulanger, P., and Letellier, L. (1992) *J. Biol. Chem.* **267,** 3173–3178
26. Feucht, A., Schmid, A., Benz, R., Schwarz, H., and Heller, K. J. (1990) *J. Biol. Chem.* **265,** 18561–18567
27. Plançon, L., Chami, M., and Letellier, L. (1997) *J. Biol. Chem.* **272,** 16868–16872
28. Lambert, O., Plancon, L., Rigaud, J. L., and Letellier, L. (1998) *Mol. Microbiol.* **30,** 761–765
29. Lambert, O., Letellier, L., Gelbart, W. M., and Rigaud, J. L. (2000) *Proc. Natl. Acad. Sci. U. S. A.* **97,** 7248–7253
30. Böhm, J., Lambert, O., Frangakis, A. S., Letellier, L., Baumeister, W., and Rigaud, J.-L. (2001) *Curr. Biol.* **11,** 1168–1175
31. Lanni, Y. T. (1960) *Virology* **10,** 501–513
32. Garnier, J., Gibrat, J. F., and Robson, B. (1996) *Methods Enzymol.* **266,** 540–553
33. Lupas, A., Van Dyke, M., and Stock, J. (1991) *Science* **252,** 1162–1164
34. Hirokawa, T., Boon-Chieng, S., and Mitaku, S. (1998) *Bioinformatics* **14,** 378–379
35. Altschul, S. F., Madden, T. L., Schaffer, A. A., Zhang, J., Zhang, Z., Miller, W., and Lipman, D. J. (1997) *Nucleic Acids Res.* **25,** 3389–3402
36. Hulo, N., Bairoch, A., Bulliard, V., Cerutti, L., De Castro, E., Langendijk-Genevaux, P. S., Pagni, M., and Sigrist, C. J. (2006) *Nucleic Acids Res.* **34,** D227–D230
37. le Maire, M., Viel, A., and Moller, J. V. (1989) *Anal. Biochem.* **177,** 50–56
38. Schagger, H., Cramer, W. A., and von Jagow, G. (1994) *Anal. Biochem.* **217,** 220–230
39. Heuberger, E. H., Veenhoff, L. M., Duurkens, R. H., Friesen, R. H., and Poolman, B. (2002) *J. Mol. Biol.* **317,** 591–600
40. Ludtke, S. J., Baldwin, P. R., and Chiu, W. (1999) *J. Struct. Biol.* **128,** 82–97
41. Rigaud, J. L., Mosser, G., Lacapere, J. J., Olofsson, A., Levy, D., and Ranck, J. L. (1997) *J. Struct. Biol.* **118,** 226–235
42. Glauner, B. (1988) *Anal. Biochem.* **172,** 451–464
43. Zweig, M., and Cummings, D. (1973) *Virology* **51,** 443–453
44. Zweig, M., and Cummings, D. (1973) *J. Mol. Biol.* **80,** 505–518
45. Katsura, I., and Hendrix, R. W. (1984) *Virology* **39,** 691–698
46. Hendrix, R. W. (2003) *Curr. Opin. Microbiol.* **6,** 506–511
47. Mc Grath, S., Neve, H., Seegers, J. F., Eijlander, R., Vegge, C. S., Brondsted, L., Heller, K. J., Fitzgerald, G. F., Vogensen, F. K., and van Sinderen, D. (2006) *J. Bacteriol.* **188,** 3972–3982
48. Edmonds, L., Liu, A., Kwan, J. J., Avanessy, A., Caracoglia, M., Yang, I., Maxwell, K. L., Rubenstein, J., Davidson, A. R., and Donaldson, L. W. (2007) *J. Mol. Biol.* **365,** 175–186
49. Del Angel, V. D., Dupuis, F., Mornon, J. P., and Callebaut, I. (2002) *Biochem. Biophys. Res. Commun.* **293,** 1153–1160
50. Moller, J. V., and le Maire, M. (1993) *J. Biol. Chem.* **268,** 18659–18672
51. Boulanger, P., le Maire, M., Bonhivers, M., Dubois, S., Desmadril, M., and Letellier, L. (1996) *Biochemistry* **35,** 14216–14224
52. Brussow, H., and Hendrix, R. W. (2002) *Cell* **108,** 13–16
53. Pedulla, M. L., Ford, M. E., Houtz, J. M., Karthikeyan, T., Wadsworth, C., Lewis, J. A., Jacobs-Sera, D., Falbo, J., Gross, J., Pannunzio, N. R., Brucker, W., Kumar, V., Kandasamy, J., Keenan, L., Bardarov, S., Kriakov, J., Lawrence, J. G., Jacobs, W. R., Jr., Hendrix, R. W., and Hatfull, G. F. (2003) *Cell* **113,** 171–182
54. Hendrix, R. W. (1988) *Curr. Top. Microbiol. Immunol.* **136,** 21–29
55. Katsura, I. (1990) *Adv. Biophys.* **26,** 1–18
56. Roessner, C. A., Struck, D. K., and Ihler, G. M. (1983) *J. Biol. Chem.* **258,** 643–648
57. Roessner, C. A., Struck, D. K., and Ihler, G. M. (1983) *J. Bacteriol.* **153,** 1528–1534
58. Katsura, I., and Kuhl, P. W. (1975) *J. Mol. Biol.* **91,** 257–273

59. Xu, D., Baburaj, K., Peterson, C. B., and Xu, Y. (2001) *Proteins* **44,** 312–320
60. Letellier, L. (1998) in *Lipid and Protein Traffic: Pathways and Molecular Mechanisms* (Op den Kamp, J. A. F., ed) Vol. 106, pp. 267–282, Springer-Verlag Inc., New York
61. Kanamaru, S., Leiman, P. G., Kostyuchenko, V. A., Chipman, P. R., Mesyanzhinov, V. V., Arisaka, F., and Rossmann, M. G. (2002) *Nature* **415,** 553–557
62. Stojkovic, E. A., and Rothman-Denes, L. B. (2007) *J. Mol. Biol.* **366,** 406–419
63. Moak, M., and Molineux, I. (2004) *Mol. Microbiol.* **51,** 1169–1183
64. Piuri, M., and Hatfull, G. F. (2006) *Mol. Microbiol.* **62,** 1569–1585
65. Heusterspreute, M., Ha-Thi, V., Tournis-Gamble, S., and Davison, J. (1987) *Gene* (*Amst.*) **52,** 155–164